CCAMLR Science, Vol. 10 (2003): 91–100

SHORT NOTE

MAXIMUM ENTROPY RECONSTRUCTIONS OF KRILL DISTRIBUTION AND ESTIMATES OF KRILL DENSITY FROM ACOUSTIC SURVEYS AT SOUTH GEORGIA, 1996–2000

M.H. Wafy and A.S. Brierley✉
Pelagic Ecology Research Group
Gatty Marine Laboratory
University of St Andrews
Fife KY16 8LB, United Kingdom
Email – asb4@st-and.ac.uk

S.F. Gull
Astrophysics Group
Cavendish Laboratory
Madingley Road
Cambridge CB3 0HE, United Kingdom

J.L. Watkins
Biosciences Division
British Antarctic Survey
High Cross, Madingley Road
Cambridge CB3 0ET, United Kingdom

Abstract

This paper presents Maximum Entropy (MaxEnt) reconstructions of krill distribution and estimates of mean krill density within two survey boxes (dimensions 80 km × 100 km) north of South Georgia. The reconstructions were generated from line-transect acoustic survey data gathered in the boxes during austral summers from 1996 to 2000. Krill densities had previously been determined at approximately 0.5 km intervals along each of the ten 80 km transects in each box, providing about 1 600 density estimates per box. The MaxEnt technique uses an iterative Bayesian approach to infer the most probable krill density for each of the 32 000 0.5 × 0.5 km cells in each box, taking explicit account of the spatial relationship between densities in the observed data. Despite some very large interannual and regional differences in mean krill density, the MaxEnt approach works well, providing plausible maps of krill distribution. The maps reveal some consistent 'hot spots' of krill distribution, knowledge of which could aid the understanding of mechanisms influencing krill distribution, and hence krill/predator interactions. The MaxEnt technique also yields mean krill densities for each survey, for which the confidence limits are often narrower than those determined from conventional statistical analyses.

Résumé

Ce document présente des reconstructions de l'entropie maximale (MaxEnt) de la répartition du krill et des estimations de la densité moyenne du krill dans deux rectangles d'étude (dimensions : 80 km × 100 km) au nord de la Géorgie du Sud. Les reconstructions sont effectuées à partir de données de radiales de campagnes d'évaluation acoustique collectées dans ces rectangles pendant les étés australs de 1996 à 2000. Par le passé, les densités de krill avaient été déterminées à des intervalles d'environ 0,5 km le long de chacune des dix radiales de 80 km de chaque rectangle qui, chacun, fournissait environ 1 600 estimations de densité. La technique de MaxEnt utilise une approche bayésienne

térative pour inférer la densité de krill la plus probable pour chacune de 32 000 cases de 0,5 x 0,5 km de chaque rectangle, et tient compte explicitement de la relation spatiale entre les densités des données observées. Malgré des différences interannuelles et régionales importantes dans la densité moyenne de krill, l'approche de MaxEnt donne de bons résultats et fournit des cartes plausibles de répartition du krill. Les cartes révèlent des points de forte concentration constante de krill dont la connaissance pourrait élucider les mécanismes influençant la répartition du krill et, de là, les interactions krill/prédateurs. La technique de MaxEnt fournit de plus, pour chaque campagne, des densités moyenne de krill dont les intervalles de confiance sont souvent plus restreints que ceux déterminés par des analyses statistiques conventionnelles.

Резюме

Статья посвящена применению метода максимума энтропии (MaxEnt) для восстановления пространственного распределения криля и оценке средней плотности криля в двух съемочных ячейках (размером 80 км × 100 км), лежащих к северу от Южной Георгии. Для восстановления использовались данные по линейным разрезам акустических съемок, собранные в этих ячейках в течение австрального лета с 1996 по 2000 г. Плотность криля была определена ранее с интервалом около 0.5 км вдоль каждого из 10 80-километровых разрезов в каждой ячейке, что дало примерно 1600 оценок плотности на ячейку. Метод MaxEnt использует итеративный байесовский подход с тем, чтобы получить наиболее вероятную плотность криля в каждой из 32 000 клеток размером 0.5 × 0.5 км для каждой ячейки, и в явном виде учитывает пространственную взаимосвязь между плотностями в данных наблюдений. Несмотря на отдельные очень большие межгодовые и региональные различия в средней плотности криля, метод MaxEnt работает хорошо, давая правдоподобные карты распределения криля. Эти карты выявили отдельные устойчивые «горячие точки» в распределении криля, информация о которых может содействовать пониманию механизмов, влияющих на распределение криля, и, следовательно, взаимодействий между крилем и хищниками. Метод MaxEnt также дает средние значения плотности криля по каждой съемке, доверительные пределы для которых зачастую уже, чем те, которые устанавливаются при обычном статистическом анализе.

Resumen

Este documento presenta reconstrucciones de la entropía máxima (MaxEnt) de la distribución de kril y estimaciones de la densidad promedio de kril en dos áreas de estudio (rectángulos de 80 km × 100 km) al norte de Georgia del Sur. Las reconstrucciones se basaron en los datos obtenidos durante las temporadas estivales de 1996 a 2000 de los transectos lineales de las prospecciones acústicas en ambos rectángulos. La densidad de kril había sido estimada previamente cada ≈0,5 km, a lo largo de los diez transectos de 80 km en cada rectángulo, produciendo unas 1 600 estimaciones de densidad por rectángulo. La técnica de MaxEnt utiliza un enfoque Bayesiano iterativo para inferir la densidad más probable de kril para cada una de las 32 000 cuadrículas de 0,5 × 0,5 km de cada rectángulo, tomando en cuenta explícitamente la relación espacial entre las densidades de los datos observados. A pesar de algunas diferencias regionales e interanuales de gran magnitud en la densidad promedio de kril, el enfoque de MaxEnt es efectivo, y proporciona mapas admisibles de la distribución de kril. Los mapas revelan algunas "zonas álgidas" en la distribución de kril, cuyo conocimiento podría ayudar a entender los mecanismos que influyen en la distribución de kril, y por ende, en las interacciones entre el kril y sus depredadores. La técnica de MaxEnt también produce densidades de kril promedio para cada prospección, para la cual los intervalos de confianza en general son más angostos que los determinados para los análisis estadísticos más convencionales.

Keywords: acoustic survey, Bayesian, density, distribution, hot spots, krill, MaxEnt, Maximum Entropy, reconstruction, CCAMLR

INTRODUCTION

Acoustic surveys are conducted frequently to estimate the biomass and map the distribution of stocks of many pelagic species including Antarctic krill (*Euphausia superba*) (e.g. Hewitt et al., 2002). Surveys tend to be limited in terms of time, however, both because of the cost of ship time and the need to complete surveys in periods that are short compared to the rates of movement (either by active migration or passive advection on currents) of the stock (McAllister, 1998). Survey transects therefore tend to be widely spaced and data are sparse. Although such surveys provide detailed information on the distribution of stocks along transects, they reveal little of their distribution between transects. In order to map the distribution of a stock throughout the whole survey area, interpolation or other inference techniques must be used to estimate density in those parts of the survey area where direct observations have not been made (off transect). Geostatistical techniques have been used for this purpose (Rivoirard et al., 2000), but have not worked well for krill survey data because of the extremely patchy nature of krill distributions (e.g. Murray, 1996). Much krill biomass is contained in rare, high density swarms, the distributions of which are difficult to model.

Bayesian theory provides a robust framework for data analysis. It enables prior knowledge of the system under study to be exploited together with new known data (Sivia, 1996). Furthermore, Skilling (1988) has shown that probability-density functions that best correspond to the constraints of known data are those which maximise the information entropy (S). Bayesian techniques applied as Maximum Entropy (MaxEnt) have been used successfully for many years in numerous branches of physical science to reconstruct images from incomplete and noisy data, for example to reconstruct maps of distant astronomical features from radio-telescope data (Gull and Daniel, 1978). More recently, MaxEnt techniques have been applied to information obtained from commercial trawl operations to map fish distributions outside those areas for which fish abundance data were available (Lizamore, 1995; Vignaux et al., 1998). This paper reports the results of MaxEnt reconstructions of the distributions of Antarctic krill in survey boxes to the north of South Georgia, based on line-transect acoustic survey data gathered in the boxes during austral summers from 1996 to 2000.

MATERIALS AND METHODS

Acoustic Survey Data

Data were gathered by the RRS *James Clark Ross* (cruise prefix JR) during austral summers from 1996 to 1999 and by the RV *Atlantida* (cruise prefix ATLD) in 2000 as a component of the British Antarctic Survey's Core Programme (Brierley et al., 1997). Details of survey design, acoustic data processing, and results as determined by Jolly and Hampton (1990) and other analyses, are given by Brierley and colleagues (Brierley et al., 1997; Brierley et al., 1999; Brierley and Goss, 1999; Sushin et al., 2000). Generally speaking, the surveys resulted in estimates of krill density every 0.5 km along each 80 km survey transect. The objective of each survey was to cover 10 such transects per box (providing 80 × 10 × 2 separate 0.5 × 0.5 km krill density estimates per box). This objective was not always achieved because of weather and/or time constraints.

MaxEnt Analysis

A full justification of the MaxEnt approach is beyond the scope of this short note. Numerous textbooks detail the underlying theory (e.g. Sivia, 1996; Wu, 1997), and Brierley et al. (2003) describe the application of the technique to analysis of line-transect acoustic survey data. The approach is Bayesian and generates the most-probable inference of the mean krill density (g m^{-2}) in each of the 32 000 0.5 × 0.5 km cells within each survey area, and provides an estimate of the standard deviation about the mean for each cell. The process is iterative and uses computer-power to progress from a user-controlled starting point to converge on a reconstruction that is most consistent with the observed data and for which the entropy is maximised. The approach has a long history of successful application in the analysis and reconstruction of sparse and noisy physical data (e.g. Gull and Daniel, 1978) and is founded on the bedrock of probability theory. It has been said that the MaxEnt approach is the only inference process that is consistent with common sense (Paris, 1994). The MaxEnt technique offers an advantage over geostatistical/kriging approaches in that it provides a probability value for each possible solution (the Bayesian *evidence*: evidence as given here is the product of $\log_e$[probability of inferred cell krill density] for all cells per survey box). This enables different reconstruction scenarios to be compared quantitatively.

An illustration often used to describe the mechanism of MaxEnt image reconstruction from limited data (e.g. Lizamore, 1995; Sivia, 1996) is the work of an imaginary team of monkeys (or scientists) throwing luminous balls (in this case krill) at random into the pixels (in this case 0.5 × 0.5 km cells) of the image (this survey area). This produces an image in which the pixel brightness (in this case inferred krill density) is

determined by the number of luminous balls in that pixel. If the monkeys repeat the process many times, many images will be produced and these can all be compared to the data. Most of the monkeys' images will not be consistent with the data and can be ignored. All the images that do fit the data can be sorted into piles of images that are the same, and the largest pile will contain the most likely inference of the image from which the data were drawn. The image produced most often by the monkeys will have the most uniform intensity and therefore the monkeys' combined efforts will have resulted in the most uniform image (the image with maximum entropy) that is consistent with the observed data.

The starting point (the Bayesian *prior*) for all 32 000 cells is set to be the mean krill density for the survey, as determined using a Jolly and Hampton (1990) analysis. The solution is constrained by the observed data in the sense that the solution is sought with minimum misfit between the observed data and reconstructed data. The entropy (S) is evaluated as

$$S(\mathbf{h}) = -\sum_{1}^{32000}\left(h(x_i) - m(x_i) - h(x_i)\log\frac{h(x_i)}{m(x_i)}\right)$$

where $h(x_i)$ is the observed krill density at a particular 0.5×0.5 km cell location x_i (a location in two dimensions, latitude and longitude) and $m(x_i)$ is the inferred krill density at the same location.

The MemSys5 data analysis package (Gull and Skilling, 1999) has been used to carry out these MaxEnt analyses. The package is able to take full account of the spatial correlation in the observed survey data and therefore exploits a valuable component of line-transect survey data that is ignored by more conventional (e.g. Jolly and Hampton, 1990) analyses. Spatial correlations are included in the MaxEnt analysis via the Intrinsic Correlation Function (ICF) technique (Gull and Skilling, 1999), in which the general idea is to build a final 'visible' reconstruction from a stacked series of 'hidden' reconstructions. The reconstruction that is compared to the data (the so-called 'visible' reconstruction) is a blurred version of the hidden one. If there is not much support for detailed features in the data, then blurring the hidden reconstructions reduces the number of available degrees of freedom and the evidence rises. If the blurring is taken too far then the likelihood is reduced so that the evidence falls. Several scales (N scales) can be included so that the reconstruction may be smooth in one area (similar krill densities in adjacent cells) and sharp elsewhere (discrete krill swarms). This approach has become known as pyramid maximum entropy (Bontekoe et al., 1994). A series of up to seven hidden reconstructions (N scales = 7), each blurred by a further linear factor of 2 (ICF widths 0, 1, 2, 4, 8, 16 and 32) and weighted by a factor of 4, was used. The ICF widths are widths of Gaussian filters and, very roughly, the number of adjacent 0.5 km cells that were correlated by ICF widths 1, 2, 4, 8, 16 and 32 were respectively 0, 1, 2, 5, 9 and 18. The final visible space reconstruction was formed by weight-summing the hidden reconstructions by convolution. Fuller details of the ICF techniques are given by Brierley et al. (2003).

Investigation of Reconstruction Accuracy

To assess how effective the MaxEnt approach was at inferring individual cell densities in the absence of observed data, 52 data points were removed at random from the raw data prior to one analysis of one cruise (JR38W). After reconstruction in the absence of these data, the MaxEnt-generated points at these positions were compared with the observed data.

RESULTS

Reconstructed maps of krill distribution are shown for the western and eastern survey boxes in Figure 1. All maps are at N scales = 6, apart from ALTDW which is at N scales = 7. Mean krill densities for each reconstruction are given in Table 1, along with coefficients of variation (CV) and equivalent values determined previously from Jolly and Hampton (1990) analyses. Also shown are the Bayesian evidence values for each reconstruction.

Comparison of the 52 observed values removed from the JR38W raw data prior to analysis with the 52 inferred by MaxEnt for the same geographic location provided support for the power and validity of this approach. A paired sample t-test failed to detect any significant difference between the observed and reconstructed data ($t = 1.8$, df = 51, $p > 0.05$).

DISCUSSION

The MaxEnt approach has produced most-probable maps of the distribution of krill in the survey areas within the constraints of the observed data. The fact that the analysis conducted in the absence of some raw data produced reconstructed values that were not significantly different from the observed data provides evidence that the inference process is robust. Some features of the

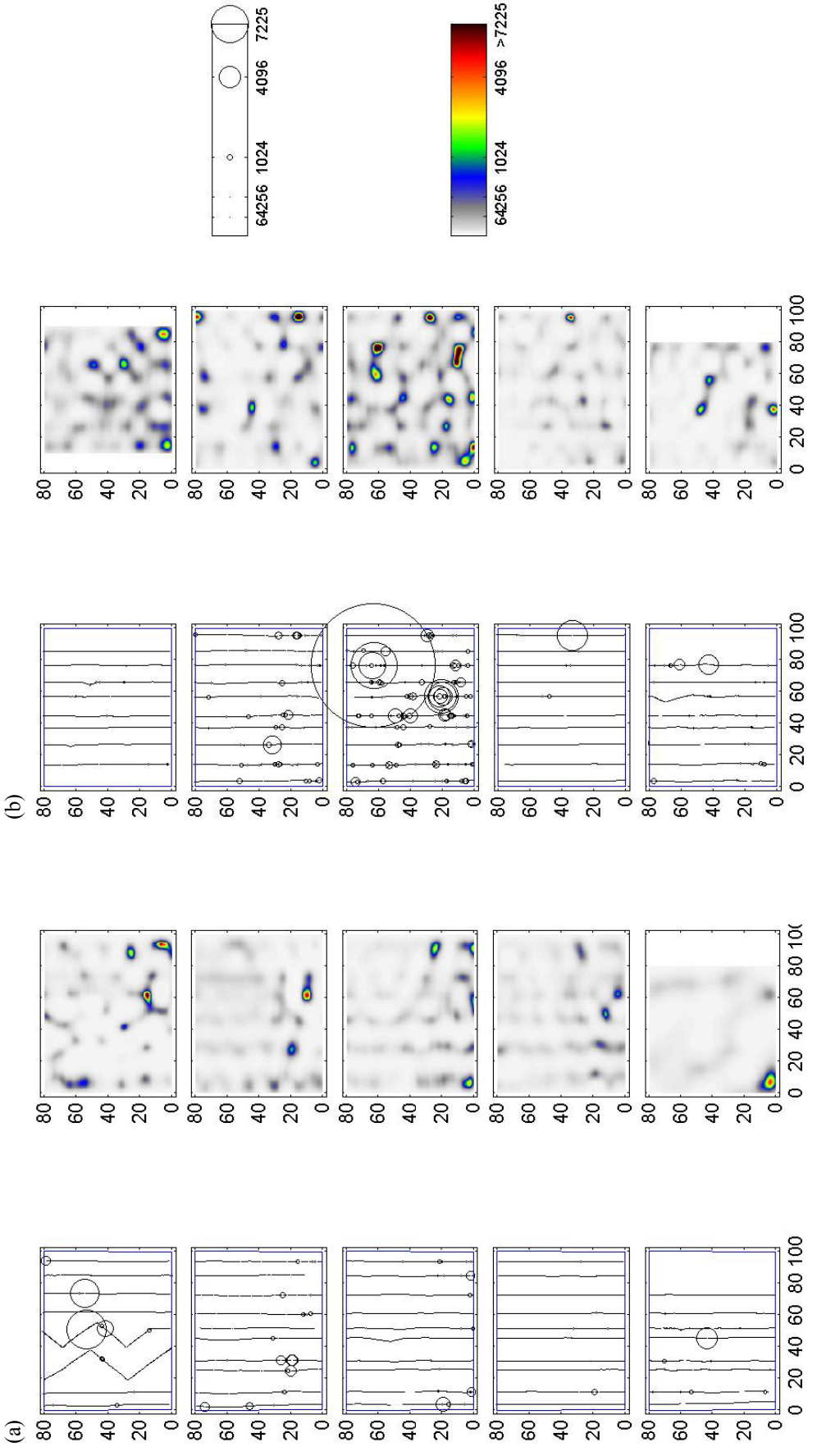

Figure 1: (a) Western survey box and (b) eastern survey box. Maps showing along-transect krill densities (left panes) and MaxEnt reconstructions of krill distribution (right panes) for (from top to bottom) JR11 (1996), JR17 (1997), JR28 (1998), JR38 (1999) and ATLD (2000). Axes are labelled in km. Scale bars show along-transect krill density (circle size is proportional to mean krill density in 0.5 km integration interval) and MaxEnt inferred krill density for each of the 0.5 × 0.5 km squares in the box (colourscale mapped to square root transformations of inferred cell density). For both scales the units are krill density, g m^{-2}.

Table 1: Mean krill densities and measures of uncertainty for acoustic surveys in the western and eastern survey boxes from 1996 to 2000. Jolly and Hampton (1990) values are derived from transect values (usually 10 but 8 for JR11 and ATLD), whereas MaxEnt values are for 32 000 0.5 × 0.5 km cells (except for JR11E and ATLD where, because only eight transects were surveyed, n = 25 600). No evidence value is available for JR17W because, for this cruise, it was not possible to satisfy all the conditions for a MaxEnt solution.

Cruise	Year	Box	Jolly and Hampton			MaxEnt			
			Mean ($g\ m^{-2}$)	Variance	CV (%)	Mean ($g\ m^{-2}$)	Variance	CV (%)	Evidence
JR11	1996	West	26.72	59.00	28.75	35.70	9.22	8.51	-1139
JR11	1996	East	40.57	13.40	9.02	54.94	30.17	10.00	-1040
JR17	1997	West	25.17	18.44	17.06	19.9	6.88	13.19	-------
JR17	1997	East	54.65	36.55	11.06	51.26	13.39	7.14	-1869
JR28	1998	West	21.41	17.96	19.79	22.08	13.18	8.47	-841
JR28	1998	East	150.99	879.68	19.64	159.34	43.10	4.12	-2186
JR38	1999	West	12.03	2.14	12.16	11.81	8.51	24.70	-475
JR38	1999	East	11.18	17.46	37.37	10.73	5.41	21.69	-725
ATLD	2000	West	12.26	10.15	25.99	24.73	7.74	3.67	-1220
ATLD	2000	East	32.70	49.54	21.52	24.37	7.08	10.92	-1792

reconstructions, however, require explanation. Banding features parallel to the transect lines are apparent for some surveys, particularly on the western side of the west survey box when the mean krill density was low. The banding arises from a combination of along-track observed krill density and transect spacing. Transects were defined using a two-stage pseudo-randomisation process (see Brierley et al., 1997). This caused transects in the west of the western core box to be more widely spaced than the average transect spacing. This wide spacing and the low along-transect density values gives rise to regions for which it is difficult to make inference. Banding is less apparent in the reconstruction of JR11W. For that cruise, bad weather prevented the usual straight transects from being surveyed and a zigzag course was adopted. This resulted in a more even spread of survey effort across the box and a better reconstruction: for mapping purposes zigzag courses appear to be superior to parallel lines. Banding is not apparent in the reconstruction of ATLDW even though the transect spacing there was the same as for previous cruises. Evidence values for ATLDW suggested that for this cruise the inclusion of longer-range spatial correlations (N scales = 7) than those considered in JR W cruises (N scales = 6) was significant. This in turn leads to a smoother image.

The best evidence value was for the reconstruction of JR38W. The distribution of (log) density for this cruise was narrow and unimodal and was consequently modelled well by the MaxEnt process. For cruises with higher mean density, such as JR28E, the evidence was lower. The distribution of (log) density became more bimodal with increased mean density (i.e. more large krill swarms were detected) and presented increasingly difficult challenges to the MaxEnt reconstruction. Geostatistical analyses of krill surveys have encountered problems with bimodal density distributions (e.g. Murray, 1996). As Sivia (1996) has pointed out, multi-modal data are difficult to model, particularly if the modes are of similar sizes (as in JR11E). For surveys where the distribution of (log) density is multi-modal, but for which the modes are of different sizes, Markov Chain Monte Carlo analyses may offer a solution; it will be investigated in the future. The relationship between total krill biomass in each survey box and the distribution of 0.5 × 0.5 km density values should be investigated further. The shape of this distribution has an influence mathematically on the variance associated with the MaxEnt reconstruction. Biologically, it would appear that the increasing bimodality of (log) density distribution occurs because when the mean krill density is high the number of very large swarms increases.

Although there are some very large differences in mean krill density between years (ranging from 36 to 12 g m^{-2} in the west and 159 to 11 g m^{-2} in the east; see Table 1), there is evidence of some consistent features between years for each box. In the west, in three of the four years for which data are available, a krill cluster can be seen at approximately x = 90 km, y = 25 km (see Figure 1a). Similarly, in the east, for all three years when data are available, a cluster is visible at approximately x = 95 km, y = 30 km (Figure 1b). Factors contributing to the consistent appearance of krill at these 'hot spots' warrant further investigation, since they

could improve the understanding of mechanisms which drive krill aggregation. This in turn could have implications for understanding predator foraging strategies. The presence of hot spots also has implications for survey design and conventional survey analysis since their existence suggests that the distributions of krill in the boxes at South Georgia are not entirely random. The hot spots are evident despite the fact that some single high-density values apparent in the along-track data are not so prominent in the reconstructed images (for example, JR11W at y = about 55). Although single high-density values appear in the reconstructions, if the high-density values are observed to be isolated in space (i.e. appear in just one 0.5 km cell), the probability of their occurrence is low and the MaxEnt process will not populate adjacent cells in the reconstructed image with high-density values. High-density values in isolated single cells are not prominent in the reconstructed images. Conversely, there are instances when patches of high density appear in the reconstructions but are not apparent in the raw along-track data. If multiple neighbouring intervals along track are observed to contain moderately high krill densities, then the probability of high densities in unsurveyed cells off transect will be high, and these cells will be attributed high densities in the reconstruction. Moderately high densities are not prominent in the along-transect data because the diameters of the circles representing these points are small on the linear scale used (Figure 1).

Building the grids at a finer spatial scale would be one way of further improving the reconstructions. Data considered here were integrated at 0.5 km intervals along transects, primarily for historical reasons. Availability of computing power no longer constrains integration to such long intervals, and smaller intervals would increase the likelihood of detecting high densities in consecutive intervals, perhaps providing more information on spatial relationships between swarms (Kalikhman, 2001). Halving the integration interval (to 0.25 km here), however, would increase the reconstruction problem (by 2^2), and could also lead to problems of acoustic species identification. Acoustic-based species identification techniques often require backscatter data that have been averaged over several pings in order to overcome the stochastic ping-to-ping variation that occurs even between echoes from the same target species (e.g. Brierley et al., 1998).

Before the MaxEnt technique can be used routinely to analyse acoustic survey data, it is suggested that detailed comparisons should be made between reconstructions generated by MaxEnt and reconstructions using other techniques, such as 'standard' geostatistics (Rivoirard et al., 2000) and geostatistics implemented in a Bayesian manner (Omre, 1987). These comparisons should ideally be made on data obtained from virtual surveys run through simulated oceans containing very highly skewed distributions of density. Simulated data are now available (e.g. Simmonds, pers. comm.) and such comparisons are the subject of our ongoing research. Reconstructions of distributions from data gathered on 'survey' through simulated data fields would offer the ability to assess the quality of the reconstruction in regions off transect. It has not been possible to do this here because, of course, the distribution of krill off transect was unknown.

At a time when decisions with potentially major biological consequences are being made about fisheries by politicians who are not necessarily conversant with the concept of scientific uncertainty (Hutchings et al., 1997), the ability to provide robust probability values associated with various biomass scenarios could be useful. For this reason, and because of the superiority of Bayesian techniques over traditional statistical approaches (Wade, 2000) and the ability of MaxEnt to function in a data-sparse environment, the MaxEnt method illustrated here could make substantial contributions to fisheries-independent management of krill.

CONCLUSIONS

Bayesian theory applied as MaxEnt provides a powerful means for reconstructing distributions of krill throughout entire survey areas from (sparse) line-transect acoustic survey data.

The MaxEnt reconstructions provide robust estimates of krill density.

Some persistent patterns of krill distribution at South Georgia are apparent from one year to the next in the MaxEnt reconstructions. These are not immediately obvious in the acoustic line-transect data. The occurrence of such 'hot spots' may have importance for understanding krill distribution and may provide insight into the foraging behaviour of krill predators.

ACKNOWLEDGEMENTS

This MaxEnt reconstruction work was supported initially by a fellowship from Clare Hall, University of Cambridge, awarded to A.S. Brierley, and more recently by a grant from the UK's Natural Environment Research Council awarded

to A.S. Brierley and S.F. Gull. We are grateful to our colleagues on board the RRS *James Clark Ross* and the RV *Atlantida* for collecting the acoustic survey data that has been analysed here, and thank N. Williamson, P. Gasiukov and A. Garrett for helpful comments on a draft version of this paper.

REFERENCES

Bontekoe, T.R., E. Koper and D.J.M. Kester. 1994. Pyramid Maximum-Entropy images of IRAS survey data. *Astronomy and Astrophysics*, 284: 1037–1053.

Brierley, A.S. and C. Goss. 1999. Acoustic estimates of krill density at South Georgia, December/ January 1998/99. Document *WG-EMM-99/20.* CCAMLR, Hobart, Australia.

Brierley, A.S., J.L. Watkins and A.W.A. Murray. 1997. Interannual variability in krill abundance at South Georgia. *Mar. Ecol. Prog. Ser.*, 150 (1–3): 87–98.

Brierley, A.S., P. Ward, J.L. Watkins and C. Goss. 1998. Acoustic discrimination of Southern Ocean zooplankton. *Deep-Sea Res.*, II: *Topical Studies in Oceanography*, 45 (7): 1155–1173.

Brierley, A.S., J.L. Watkins, C. Goss, M.T. Wilkinson and I. Everson. 1999. Acoustic estimates of krill density at South Georgia, 1981 to 1998. *CCAMLR Science*, 6: 47–57.

Brierley, A.S., S.F. Gull and M.H. Wafy. 2003. Bayesian Maximum Entropy reconstruction of stock distribution and inference of stock density from line-transect acoustic survey data. *ICES J. Mar. Sci.*, 60 (3): 446–452.

Gull, S.F. and G.J. Daniel. 1978. Image reconstruction from incomplete and noisy data. *Nature*, 272: 686–691.

Gull, S.F. and J. Skilling. 1999. *Quantified Maximum Entropy. MemSys5 Users Manual V1.2.* www.maxent.co.uk/documents/MemSys5_manual.pdf: 99 pp.

Hewitt, R.P., J.L. Watkins, M. Naganobu, P. Tshernyshkov, A.S. Brierley, D.A. Demer, S. Kasatkina, Y. Takao, C. Goss, A. Malyshko, M.A. Brandon, S. Kawaguchi, V. Siegel, P.N. Trathan, J.H. Emery, I. Everson and D.G.M. Miller. 2002. Setting a precautionary catch limit for Antarctic krill. *Oceanography*, 15: 26–33.

Hutchings, J.A., C. Walters and R.L. Haedrich. 1997. Is scientific inquiry incompatible with government information control? *Can. J. Fish. Aquat. Sci.*, 54: 1198–1210.

Jolly, G.M. and I. Hampton. 1990. A stratified random transect design for acoustic surveys of fish stocks. *Can. J. Fish. Aquat. Sci.*, 47: 1282–1291.

Kalikhman, I. 2001. Patchy distribution fields: sampling distance unit and reconstruction adequacy. *ICES J. Mar. Sci.*, 58: 1184–1194.

Lizamore, S.C. 1995. Topics in maximum entropy applications. M.Sc. thesis, Victoria University of Wellington: 66 pp.

McAllister, M.K. 1998. Modeling the effects of fish migration on bias and variance in area-swept estimates of biomass: a vector-based approach. *Can. J. Fish. Aquat. Sci.*, 55: 2622–2641.

Murray, A.W.A. 1996. Comparison of geostatistical and random sample survey analyses of Antarctic krill acoustic data. *ICES J. Mar. Sci.*, 53: 415–421.

Omre, H. 1987. Bayesian kriging: merging observations and qualified guesses in kriging. *Mathematical Geology*, 19: 25–39.

Paris, J.B. 1994. The uncertain reasoner's companion; a mathematical perspective. *Cambridge Tracts in Theoretical Computer Science*, 39. Cambridge University Press: 212 pp.

Rivoirard, J., E.J. Simmonds, K.G. Foote, P.G. Fernandes and N. Bez. 2000. *Geostatistics for Estimating Fish Abundance*. Blackwell: 198 pp.

Sivia, D.S. 1996. *Data Analysis – a Bayesian Tutorial*. Oxford University Press: 189 pp.

Skilling, J. 1988. The axioms of maximum entropy. In: Erickson, G.J. and C.R. Smith Kluwer (Eds). *Maximum Entropy and Bayesian Methods in Science and Engineering*: 1 p.

Sushin, V.A., P.P. Chernyshkov, F.F. Litvinov, J.L. Watkins and A.S. Brierley. 2000. Krill distribution related to water structure and dynamics on the South Georgia shelf in January 2000 (AtlantNIRO–BAS Core Programme 1999/ 2000). Document *WG-EMM-00/51*. CCAMLR, Hobart, Australia.

Vignaux, M., G.A. Vignaux, S. Lizamore and D. Gresham. 1998. Fine-scale mapping of fish distribution from commercial catch and effort data using maximum entropy tomography. *Can. J. Fish. Aquat. Sci.*, 55: 1220–1227.

Wade, P.R. 2000. Bayesian methods in conservation biology. *Conservation Biology*, 14: 1308–1316.

Wu, N. 1997. The maximum entropy method. *Springer Series in Information Sciences*, 32. Springer Verlag: 327 pp.

Liste des tableaux

Tableau 1: Densités moyennes de krill et mesures de l'incertitude des campagnes d'évaluation acoustique des rectangles ouest et est de 1996 à 2000. Les valeurs de Jolly et Hampton (1990) sont dérivées des valeurs des transects (en général 10 mais 8 pour JR11 et ATLD), alors que les valeurs de MaxEnt correspondent à 32 000 cases de 0,5 × 0,5 km (sauf pour JR11E et ATLD où, comme huit radiales seulement ont été évaluées, n = 25 600). Aucune valeur évidente n'est disponible pour JR17W du fait que, pour cette campagne, il n'a pas été possible de satisfaire à toutes les conditions requises pour parvenir à une solution de MaxEnt.

Liste des figures

Figure 1: (a) Rectangle d'évaluation de l'ouest et (b) rectangle de l'est. Cartes illustrant les densités de krill le long des radiales (cadres de gauche) et les reconstructions de MaxEnt de la répartition de krill (cadres de droite) pour (de haut en bas) JR11 (1996), JR17 (1997), JR28 (1998), JR38 (1999) et ATLD (2000). Les axes sont gradués en km. Les barres d'échelle indiquent la densité de krill le long des radiales (la taille des cercles est proportionnelle à la densité moyenne de krill à des intervalles d'intégration de 0,5 km) et la densité de krill inférée par MaxEnt pour chaque case de 0,5 x 0,5 km du rectangle (les couleurs représentent les transformations de racine carrée de la densité inférée des cases). Pour les deux échelles, les unités représentent la densité de krill en g m^{-2}.

Список таблиц

Табл. 1: Средние значения плотности криля и меры неопределенности для акустических съемок в западной и восточной съемочных ячейках, 1996–2000 гг. Значения по Джолли и Хамптону (Jolly and Hampton (1990)) получены по точкам разрезов (обычно – 10, но для JR11 и ATLD – 8), а значения по MaxEnt получены для 32 000 клеток размером 0.5 × 0.5 км (за исключением JR11E и ATLD, в которых было выполнено только 8 съемочных разрезов, поэтому n = 25 600). Значений по JR17W не имеется, поскольку в случае этого рейса было невозможно удовлетворить все условия для решения по методу MaxEnt.

Список рисунков

Рис. 1: (a) Западная ячейка съемки и (b) восточная ячейка съемки. Карты, показывающие плотности криля вдоль разрезов (левая часть) и восстановление пространственного распределения криля по методу MaxEnt (правая часть) для (сверху вниз) JR11 (1996), JR17 (1997), JR28 (1998), JR38 (1999) и ATLD (2000). Оси обозначены в км. Верхняя шкала показывает плотность криля вдоль разрезов (размер кружка пропорционален средней плотности криля при интервале осреднения 0.5 км), нижняя шкала показывает плотность криля, полученную по методу MaxEnt для каждой клетки (0.5 × 0.5 км) съемочной ячейки (цветовая шкала дана как квадратный корень из полученной плотности в клетках). Для обеих шкал плотность криля выражена в г $м^{-2}$.

Lista de las tablas

Tabla 1: Promedios de la densidad de kril y mediciones de la incertidumbre de las prospecciones acústicas en los rectángulos oriental y occidental desde 1996 hasta 2000. Los valores calculados por Jolly y Hampton (1990) se derivaron de los transectos (10 transectos en general, pero 8 para JR11 y ATLD), mientras que los valores de MaxEnt se derivaron de 32 000 cuadrículas de 0,5 × 0,5 km (excepto para JR11E y ATLD donde n = 25 600 dado que sólo se analizaron ocho transectos). No se dispone de un valor para JR17W porque no fue posible satisfacer todas las condiciones para MaxEnt en esta campaña.

Lista de las figuras